ELSEVIER

Ocean Modelling 2 (2000) 109–121

Ocean Modelling

www.elsevier.com/locate/omodol

Stratified convection with multiple states

J.A. Whitehead

Woods Hole Oceanographic Institution, MS# 21, 360 Woods Hole Road, Woods Hole, MA 02543-1541, USA

Abstract

A simplified box model of the cooling of a salt-stratified ocean is analyzed analytically and numerically. A large isothermal basin of salt water has a layer of fresh water at the surface. Beside this is a small basin, cooled from above and connected to the large basin by horizontal tubes at the top, middle and bottom. For small cooling rate, fresh water enters the small basin, is cooled and leaves through the middle tube. For greater cooling rate, the fresh water leaves the small basin through the middle and bottom tube. If the top tube is smaller than the deeper tubes and the fresh water layer is sufficiently shallow, flow in the middle tube reverses at a critical cooling rate. In this case, a mixture of salt and fresh water is cooled and leaves the bottom tube. Increased cooling produces much greater flow rate; consequentially temperature increases rather than decreases in the small basin. A relaxation heat flow condition results in multiple equilibria. One of the stable modes has fresh surface water descending in the small basin and flowing out through the middle and bottom tube. The other has a greater rate of flow of both fresh and salty water (through the middle tube) into the basin with the flow of mixed salty water out of the bottom tube. Implications for deep convection in the ocean are discussed.

Keywords: Mixing; Ocean convection; Salt balance; Water circulation; Ocean circulation; Water masses

1. Introduction

Although the bulk of ocean water is colder than about 5°C, and this water is injected in the deep ocean by sinking during wintertime cooling in polar regions, it is well known that the ocean is notoriously "fickle" in its selection of deep water emplacement locations. Only a small percentage of the ocean experiences deep mixed layers that characterize deep convection (Stommel, 1962), and a list of such sites includes localities with areas at most 10^6 km^2 within the Greenland–Norwegian Sea, the Labrador Sea, the MEDOC regions in the Mediterranean, the Weddell Sea, and the Ross Sea. The total area is less than 5×10^6 km^2. A comparison with the total ocean area of 361×10^6 km^2 (Sverdrup et al., 1942) illustrates how very small the deep convection areas are.

E-mail address: jwhitehead@whoi.edu (J.A. Whitehead).

1463-5003/00/$ - see front matter
PII: S1463-5003(00)00012-3

The scarcity of such deep convection regions is due partly to the halocline that exists near the ocean surface virtually everywhere in polar regions (Sverdrup et al., 1942). Cooling of the fresher, lower-density surface water in polar regions typically leads to colder surface water and in some cases to an ice cover that limits further cooling if the cooling is great enough. The maintenance of the surface halocline throughout the Nordic Seas is maintained by freshwater accumulation (Aagaard and Carmack, 1989). Convection can penetrate to sizeable depths only if an adequate increase in density results from cooling of the stratified surface (halocline) region that typically is about 100 m deep. In addition, an increase of salinity of the water that is being cooled is required. Brine rejection by ice formation can increase the salinity of the surface halocline, but this must be maintained by wind stress that removes the ice from the region. Another source of salinity increase is the mixing of cooled fresh surface water with salty water at depth, a process that has received considerable attention recently (Legg and McWilliams, 2000). A fine view of mixed layer deepening and the formation of new Labrador Sea water as a mixture of fresher cold shallow water with deeper salty water is provided by the recent Labrador Sea deep convection experiment (Lab Sea Group, 1998). Similar observations with less details were made in the Mediterranean Sea (MEDOC Group, 1969). The same sort of deep convection is inferred for the Antarctic Ocean, with the Weddell Sea gyre being the most prominently investigated region (Gordon and Huber, 1990, 1993).

In addition to being located in a small percentage of the area of the ocean, deep convection in these regions occurs sporadically. Typically deep convection is not found every winter. Usually there are a few winters of deep convection separated by some winters of only very shallow convection. Many polynia areas in the ice-covered regions also do not appear regularly every winter. The most significant is perhaps the giant polynia that was found in the Weddell Sea in the 1970's and has not been found since.

The purpose of the present study is to present a model that emphasizes the role of the surface halocline. We describe in Section 2 a simplified model of convection in a body of salt water with a layer of fresh water on the top. The results are presented in simple analytic form. For a wide range of parameters, only the fresh surface water is cooled and sinks, and the deeper salty water remains passive. In Section 3, we investigate the behavior under the special conditions required for another mode of flow to emerge with the salty water directly included in the sinking motion. In Section 4, numerical solutions to the equations illustrate the salty mode. The transition from the fresh water mode to a salty mode results in a nonlinear relation between cooling rate and temperature. Using a relaxation rate cooling law from a cold region above the sinking region, multiple equilibria are found. Water temperature, salinity and density of the water exhibit hysteresis as temperature of the cold region above the sinking region is decreased and then increased again.

2. The cooling of surface fresh water

A confined small basin in a field of gravity cooled from above represents the convecting region. This basin is connected to a large basin (a model of the large ocean away from the location of surface cooling) with three tubes, one at the surface, one at mid-depth ($D/2$), and the third at depth D as sketched in Fig. 1. The water in the large basin has salinity S_0 and temperature T_0 except for a surface layer of fresh water of fixed depth $d < D/2$ and temperature T_0. Most

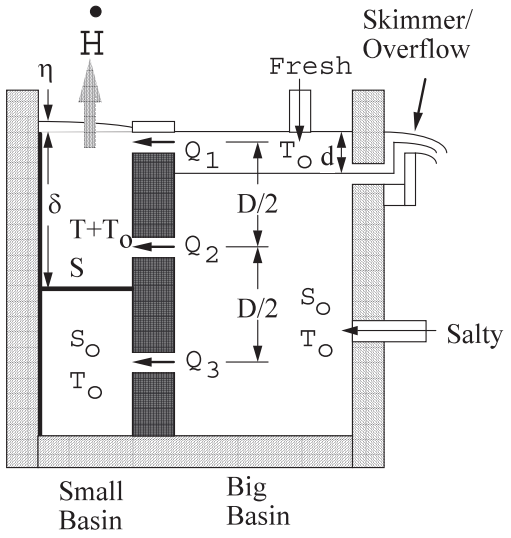

Fig. 1. Vertical cross-section of a model of a small basin with cooling next to a straitified big basin. Two layers with different salinities in the big basin are maintained by pumping in both fresh and (denser) salty water constantly at top and bottom, respectively. A skimmer/overflow removes both fresh and salty water at depth d below the surface, thus maintaining a sharp interface.

importantly, we take this large basin to be so large and so well mixed by large-scale circulation, that d, S_0, and T_0 remain fixed irrespective of the flow into and out of the tubes from the small basin. A laboratory device that could maintain such a state through the use of a skimmer is shown in Fig. 1, but again we emphasize that the intent is to duplicate an ambient salt-stratified ocean without salt-flux conditions.

In contrast to the big basin, water properties in the small basin change due to surface cooling and flow through the tubes. We assume that the upper layer water in the small basin is well mixed vertically. Since it is cooled from above, this assumption seems justified. In later solutions, salty water will flow in through the middle tube. This inflow is possible only if the cold mixed water in the small basin is denser than the salt water in the big basin. Thus the water flowing into the small basin would rise to the top as a turbulent plume and then be mixed down by surface convection. This insures that the water in the small basin remains well mixed.

In response to the surface cooling, the small basin contains a mixed layer of water of depth δ, salinity S, and temperature $T_0 + T$, where δ, S, and T are variables that must be determined. The small basin is cooled from above so that heat flux into the basin is negative and of magnitude $\dot{H}$. Thus the value of T from this cooling is negative. We neglect heat and salinity transport at the base of this layer. Consequently, for $\delta < D$ deep water with salinity S_0 and temperature T_0 lies below the layer in the small basin. Since the layer in the small basin is well-mixed and cooled, it is denser than the surface layer of fresh water in the big basin and we can anticipate that $\delta > d$.

The two basins are connected by three tubes at top, mid-depth and bottom with radii much less than d. The symbol Q_i denotes the volume flux from the large basin to the small basin through tube i, where $i = 1, 2, 3$ starting from the top. We assume there is a steady-state flow relation between Q_i and pressure difference between large and small basin of the form

$$Q_i = C_i(p_{0i} - p_i), \tag{1}$$

where p_i is pressure in the small basin and p_{0i} is pressure of the large basin. We would have, for example, $C_i = \pi r_i^4/8\mu L$ for laminar fully developed pipe flow through a tube of radius r_i and length L for fluid with viscosity μ. Other cross-section shapes would have different relations whose details are not important for this study. Here we simply retain $C_2 = C_3 = C$ to express the hydraulic resistance for tubes 2 and 3. For reasons which will become obvious later, we assign $C_1 = \gamma C$ for the hydraulic resistance of tube 1 in which $\gamma = (r_1/r_2)^4$. Using the Boussinesq approximation by assuming $\beta S, \beta S_0, |\alpha T| \ll 1$ everywhere, the pressure at tube i is determined by the hydrostatic relation

$$p_i = \rho_0 g\eta + \rho_0 g(1 + \beta S - \alpha T)D\left(\frac{i-1}{2}\right), \quad i = 1, 2, 3, \tag{2}$$

where η is the excess in surface elevation of the water surface in the small basin compared to the water surface in the large basin, and

$$\begin{aligned} p_{01} &= 0, \\ p_{0i} &= \rho_0 g d + \rho_0 g(1 + \beta S_0)\left[\left(\frac{i-1}{2}\right)D - d\right], \quad i = 2, 3. \end{aligned} \tag{3}$$

A linear equation of state has been assumed and ρ_0 is evaluated at temperature T_0. The region is thermally insulated on the sides and bottom. The water in the small basin is cooled steadily from above. It is thus mixed by convection so that T becomes uniform and negative. The interface between fresh surface water and deep water descends to a level below the middle tube. The fresh water enters the small basin through tube 1 and exits through tube 2. Thus heat flow is

$$\dot{H} = \rho_0 c_p Q_2 T. \tag{4a}$$

Assuming small cooling at this stage, so that only the top two tubes are involved, we have

$$Q_1 + Q_2 = 0 \quad \text{and} \quad -\dot{H} = \rho_0 c_p Q_1 T. \tag{4b}$$

The small basin contains a layer of fresh water, so we can use (1)–(3) to determine volume flux:

$$Q_1 = -\gamma C \rho_0 g \eta, \tag{5a}$$

$$Q_2 = C\rho_0 g\left[-\eta + \frac{\beta S_0 D}{2} + \frac{\alpha T D}{2} - \beta S_0 d\right], \tag{5b}$$

and since $Q_1 + Q_2 = 0$,

$$\eta = \frac{(\beta S_0 + \alpha T)D - 2\beta S_0 d}{2\gamma + 2}, \tag{6}$$

so that

$$Q_1 = -Q_2 = -\frac{\gamma C \rho_0 g[(\beta S_0 + \alpha T)D - 2\beta S_0 d]}{2\gamma + 2}. \tag{7}$$

Even in the limit of very small cooling, temperature must be lower than size $T_{\rm nil} = -\beta S_0[1 - 2d/D]/\alpha$ for steady flow. For greater intensity of cooling, temperature decreases and Q_1 (>0) increases linearly with departure of temperature from $T_{\rm nil}$. Note that for all cases $\eta < 0$ so the surface fluid flows from the big basin into the small basin as expected.

Zero flow through tube 3 is required by continuity of the deep fluid, so hydrostatic pressure at both sides of the tube matches in the deep fluid. Recall that heat transfer and mixing downward through the base of the layer is ignored. This dictates that the depth δ of the cooled layer is

$$\delta = \frac{1}{1+\gamma}\left[\frac{D}{2} + \frac{\beta S_0 d\gamma}{\alpha T + \beta S_0}\right]. \tag{8}$$

The cooled layer interface reaches the third tube for $\delta = D$, which defines a 'critical' temperature of

$$\alpha T_{\rm c} = -\beta S_0\left[1 - \frac{2d\gamma}{D(1+2\gamma)}\right]. \tag{9}$$

For colder temperature, the flows through all three tubes must be considered. Since Q_2 is negative for $\delta \to D^-$, we first ask whether this continues, so that the cooled region continues to be filled with only fresh water. Allowing $S \neq 0$ and using $Q_1 + Q_2 + Q_3 = 0$, it is readily shown that $\eta = (3A - 4B)/2(2+\gamma)$ so that

$$Q_1 = \frac{\gamma C\rho_0 g}{2+\gamma}\left[-\frac{3}{2}A + 2B\right], \tag{10}$$

$$Q_2 = \frac{C\rho_0 g}{2+\gamma}\left[\frac{\gamma-1}{2}A - \gamma B\right], \tag{11}$$

$$Q_3 = \frac{C\rho_0 g}{2+\gamma}\left[\frac{1+2\gamma}{2}A - \gamma B\right], \tag{12}$$

where

$$A = (\beta S_0 + \alpha T - \beta S)D \tag{13a}$$

and

$$B = \beta S_0 d. \tag{13b}$$

Setting $T = T_{\rm c}$ it is readily seen that Eqs. (10)–(12) agree with Eq. (7) for two tubes, so that $Q_1 = -Q_2$ and flow in the third tube is zero. Thus for $T = T_{\rm c}$ no salt water flows into the small basin so that $S = 0$. The value of the interface elevation is greater than D for greater cooling and will be not required. Thus the fate of the fluid trapped in the confined region below the third tube in the small basin is not of interest.

With values of $\gamma \geqslant 1$, Eq. (10) shows that with $S = 0$ the positive flow Q_1 becomes larger as T becomes more negative starting from $T_{\rm c}$. Eq. (11) shows that Q_2 which is negative becomes more so, and Q_3 becomes negative starting from zero. Thus, the small basin always stays filled with fresh water. Localized cooling causes the sinking of surface fresh water and only this cold surface

water is exported to the adjacent big basin. In no case is the deep salty water directly cooled by surface cooling. For $\gamma \geqslant 1$, this trend continues indefinitely with increased cooling rate. Such cases are not of further interest.

3. Cooling of deep salty water

Section 2 shows that for $\gamma \geqslant 1$ surface cooling results in colder fresh water and does not involve the cooling of salt water. Conversely, for $\gamma < 1$, the salinity is easily seen to become important in the small basin for the following reason. Eq. (11) shows that Q_2 which is negative becomes *less* so with more negative T. Note that Q_1 and Q_3 keep the same signs as in Section 2. Thus, for progressively more cooling (hence, more negative T), there is a value where $Q_2 = 0$. At this point, where from (11) $A = 2\gamma B/(\gamma - 1)$, we define a second critical temperature

$$T_{cc} = \frac{\beta S_0}{\alpha}\left[\frac{2\gamma d}{(\gamma - 1)D} - 1\right], \tag{14}$$

where the governing equations change because we must include a salinity balance in the small basin. Note that for $\gamma < 1$, $T_{cc} < 0$ as required and it becomes minus infinity for $\gamma \to 1^-$. Thus a finite negative value of temperature is insufficient to produce this limit for $\gamma = 1$ and the results are consistent with those in Section 2.

Heat flux can be calculated using (4b) since only the surface tube has inflow into the region. Using this with (10), (13a), (13b), and (14), the heat flow needed to produce this critical temperature is

$$\dot{H} = \frac{\rho_0^2 \gamma c_p C g d[(1-\gamma)D + 2\gamma d]\beta^2 S_0^2}{\alpha(1-\gamma)^2 D}. \tag{15}$$

So far, the system has had monotonically increasing flow rate with cooling so consequently the system behaves like many simple convecting flows. For greater cooling rates the behavior of interest begins. For flows with $Q_2 > 0$ there is an inflow of salty water into the small basin. We assume that this completely mixes with the water in the top cooled layer to produce water of salinity S. Such mixing will be aided by the cooling from above in the small basin. Also, since the water in the small basin is denser than the salt water flowing in through tube 2, the salt water would rise to the surface as a turbulent plume and thus mix. The mixing would also be enhanced by cooling from above, so we will continue assuming that the water in the small basin is well mixed. Thus conservation of salt dictates that

$$Q_2 S_0 + Q_3 S = 0, \tag{16}$$

so that using (11) and (12)

$$A = \frac{2\gamma(S_0 + S)B}{(1+2\gamma)S - (1-\gamma)S_0}. \tag{17}$$

The expressions for volume flux are simply expressed as

$$Q_1 = E(S - S_0), \tag{18}$$

$$Q_2 = -ES, \tag{19}$$

$$Q_3 = ES_0, \tag{20}$$

where

$$E = \frac{C\gamma\rho_0 g\beta S_0 d}{[(1+2\gamma)S - (1-\gamma)S_0]}. \tag{21}$$

Note that volume flux using (18)–(20) with $S = 0$ agrees with the critical volume flux from (10)–(14) with $S = 0$. Note also that for $\gamma < 1$ and $S \ll S_0$, E is negative so $Q_1 > 0,\ Q_2 > 0,\ Q_3 < 0$ for any nonzero S as required.

Setting (10)–(12) equal to (18)–(20) produces expressions linking S and T. The relation is more simply seen by defining $T' = T - T_{cc}$. Eq. (17) with (13a) and (13b) then gives

$$\alpha T' = \beta S\left[1 - \frac{2\gamma d(\gamma+2)S_0}{D(1-\gamma)[(1-\gamma)S_0 - (1+2\gamma)S]}\right]. \tag{22}$$

Converting the portion in large square brackets to a fraction, the numerator of the right-hand side is quadratic in S so that two values of S may exist for the same value of T'.

As the inflow through the mid-depth tube increases, S progressively increases from zero. Eq. (22) shows that for d/D arbitrarily small T' first begins to increase for $\gamma < 1$. There is a switch from convection retarded by fresh water in the small basin to convection with considerably less retardation by the salt and fresh water mixture in the small basin. Consequently, a decrease in T accompanies a salinity increase. The bulk density of the water in the small basin increases through salinity increase even though temperature becomes warmer. Heat flow is governed by

$$-\dot{H} = \rho_0 C_p |Q_3| T = \frac{\rho_0^2 C_p C d\gamma g\beta S_0^2 T}{[(1+2\gamma)S - (1-\gamma)S_0]} \tag{23}$$

which gives a linear relation between S and T for fixed heat flux. We see that as

$$S \to \frac{(1-\gamma)S_0}{1+2\gamma}, \quad T' \to -\infty \quad \text{and} \quad \dot{H} \to -\infty.$$

The relation between volume flux and temperature difference for $\gamma < 1$ is easily summarized visually using the sketch in Fig. 2. Starting with small cooling, temperature is below T_{nil} and there

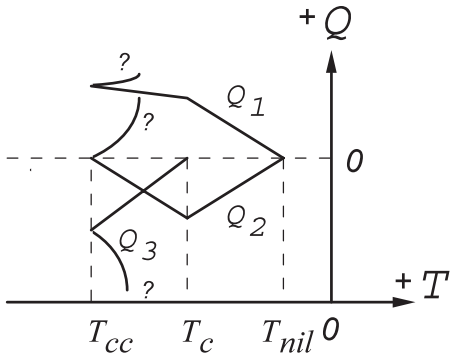

Fig. 2. Sketch of the relation between T and volume fluxes of the three tubes.

is inflow through the top tube with an equal amount of outflow through the middle tube. For $T_{cc} < T < T_c$ there is outflow in both middle and bottom tube, but magnitude of flow through the middle tube decreases with T. For these two cases, flow magnitudes are linear with T. At $T = T_{cc}$ the outflow in the middle tube becomes zero. For greater cooling, $Q_2 > 0$ so the salty water flows into the small basin. The temperatures begin to increase and the magnitudes are no longer linear with T. The curves in Fig. 2 are terminated in question marks as the trajectories are solutions of complicated polynomials. This motivated the numerical studies presented in the following section.

4. Numerical solutions

Since the calculations in Section 3 become complicated, the solutions were determined numerically. The equations were cast in dimensionless form using the transformations

$$\tilde{Q} = \frac{Q}{Q_s}, \quad Q_s = \frac{\gamma C \rho_0 g \beta S_0 D}{2+\gamma}, \quad \tilde{T} = \frac{\alpha T}{\beta S_0}, \quad \tilde{d} = \frac{d}{D}, \quad \tilde{S} = \frac{S}{S_0},$$

where subscript s denotes the volume-flux scale. The equivalent of Eq. (7) is

$$\tilde{Q}_1 = -\tilde{Q}_2 = \frac{2+\gamma}{2+2\gamma}(1 + \tilde{T} - 2\tilde{d}) \tag{24}$$

and Eqs. (10)–(12) transform to

$$\tilde{Q}_1 = -\frac{3}{2}[1 + \tilde{T} - \tilde{S}] + 2\tilde{d}, \tag{25a}$$

$$\tilde{Q}_2 = \frac{1-\gamma^{-1}}{2}[1 + \tilde{T} - \tilde{S}] - \tilde{d}, \tag{25b}$$

$$\tilde{Q}_3 = \frac{2+\gamma^{-1}}{2}[1 + \tilde{T} - \tilde{S}] - \tilde{d}. \tag{25c}$$

The scaled heat and salt balances in the small basin are governed by time-dependent counterparts to (4b) (using $\tilde{Q}_2$ and $\tilde{Q}_3$) and (16):

$$\frac{d\tilde{T}}{d\tilde{t}} = -\tilde{H} + \tilde{T}[\tilde{Q}_1 \Gamma(-\tilde{Q}_1) + \tilde{Q}_2 \Gamma(-\tilde{Q}_2) + \tilde{Q}_3 \Gamma(-\tilde{Q}_3)], \tag{26a}$$

$$\frac{d\tilde{S}}{d\tilde{t}} = \tilde{Q}_2[\tilde{S}\Gamma(-\tilde{Q}_2) + \Gamma(\tilde{Q}_2)] + \tilde{Q}_3[\tilde{S}\Gamma(-\tilde{Q}_3) + \Gamma(-\tilde{Q}_3)], \tag{26b}$$

where the timescale is AD/Q_s, the heat-flux scale is $\rho c_p T_s Q_s$, and $T_s = \beta S_0/\alpha$.

Numerical experiments were first conducted by setting a value for $\tilde{H}$ ($\ll 1$) and integrating (26a) and (26b) using (25a)–(25c) with time until they converged to a fixed value as defined below. Each integration was repeated while gradually increasing $\tilde{H}$ for a few hundred increments. To

insure that solutions converged with time to single values, the calculations were also conducted while decreasing $\tilde{H}$ over the same range. Sufficient time steps were used so that the difference in the trajectories was less than a line width (about 10^{-4} of the full range) over a wide range of parameters ($0 < \tilde{H} < 2$, $\tilde{d} < 0.5$, $\gamma < 1.0$). The flow exhibited all the features described in the text up to Eq. (23) including a transition from shallow to deep flow and the introduction of salt water into the small basin, but there were no discrete jumps in properties for any of the calculations. A typical result is shown in Fig. 3.

From results like Fig. 3, it is safe to conclude that there are no multiple valued solutions in this problem as formulated up to this stage. In contrast, when the above sequence of calculations was repeated using the heat-flux relation

$$\tilde{H} = K(\tilde{T}^* - \tilde{T}) \tag{27}$$

multiple equilibria were found. One can see that why this relation works using Fig. 3, since with the proper selection of constant K the heat flow curve, which is a straight line, will intersect the curve in Fig. 3 at three locations.

Eq. (27) increases the number of dimensionless numbers to three, so for simplicity in the initial calculations, we use the constant $K = 1$. We found that the solutions converged to multiple values for small values of $\tilde{d}, \gamma$. Fig. 4 shows trajectories for solutions in the range $-1.7 < \tilde{T}^* < -0.4$, with three different values of $\tilde{d}$ and γ, $(0.05, 0.05)$, $(0.05, 0.35)$, and $(0.05, 0.5)$. To obtain these curves, the value of $\tilde{T}^*$ was slowly decreased downward 350 times, integrating (26a) and (26b) and 150 time steps of size 0.001 between each change in value. Then, the value of $\tilde{T}^*$ was slowly increased for the same increments.

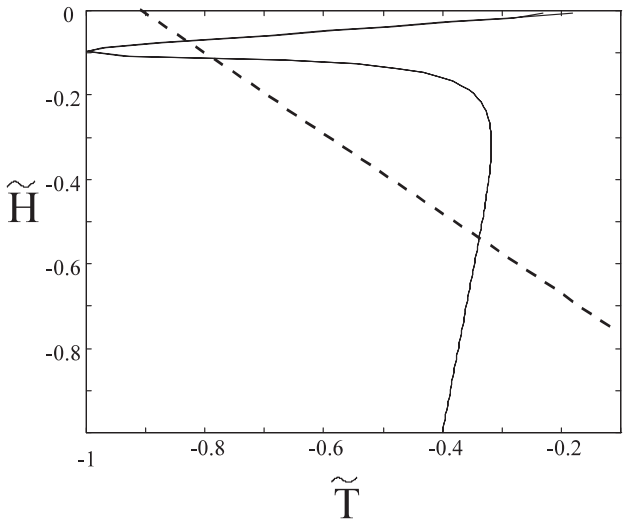

Fig. 3. Relation between heat flux and temperature of the cooled fluid for the case with of $\tilde{d}, \gamma = (0.05, 0.05)$. The solution was obtained numerically by increasing heat flux by small increments over the range shown and then by decreasing heat flux by small increments over the same range. The results lie almost exactly over each other. The dashed line illustrates a relaxation condition that produces multiple equilibrium in this model.

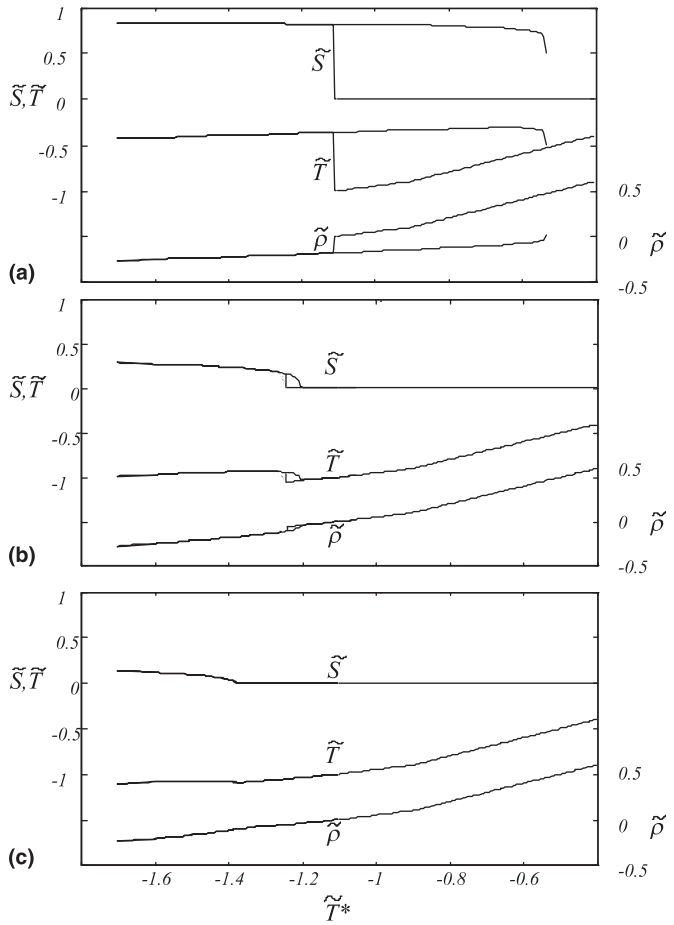

Fig. 4. Solutions for $\tilde{S},\tilde{T},\tilde{\rho}=1+\tilde{T}-\tilde{S}$ (top to bottom) to Eqs. (24)–(27) for the cases (a) $\tilde{d},\gamma=(0.05,0.05)$, (b) $(0.05,0.35)$, and (c) $(0.05,0.50)$, respectively.

The top panel in Fig. 4 shows a typical example of results in a range where there are pronounced multiple equilibria. Many such curves were found for parameters slightly different than those with $\tilde{d},\gamma \ll 1$. As the independent variable $\tilde{T}^*$, decreases from a value of -0.4, the temperature and consequently the density decreases almost linearly with $\tilde{T}^*$. First two and then, at a change in slope, three tubes are involved in the convection. At a critical value, salinity jumps to a finite size. Simultaneously temperature jumps up by a smaller amount (everything scaled), so that density jumps down. Then upon further decrease in $\tilde{T}^*$, salinity increases and temperature and density decrease slightly. As the process is reversed, that is as $\tilde{T}^*$ is increased again from a value of -1.7, the values repeat themselves except that the trajectory continues beyond the "jump" point. Finally a lower value of $\tilde{T}^*$ is reached where the curves jump back to the case with $\tilde{S}=0$. Close to transition back to the fresh mode there is a steep decline in salinity and increase in temperature with a less abrupt change in density. We surmise that in that region there must be substantial balancing of thermal and salinity effects.

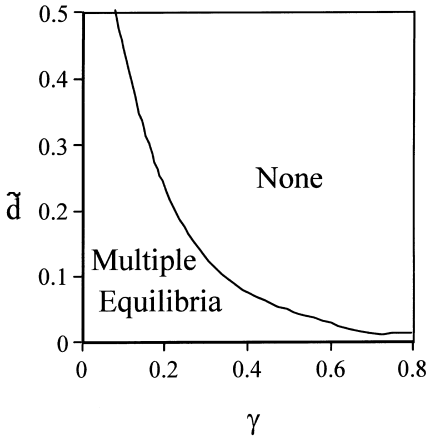

Fig. 5. Region in parameter space for multiple equilibria.

For the values $\tilde{d}, \gamma = (0.05, 0.35)$ the range of hysteresis is much smaller. Salinity and temperature jump by a small amount at the point of transition, and as in the case of (a) density jump is smaller than the scaled temperature and salinity jumps. For the values of $\tilde{d}, \gamma = (0.05, 0.50)$ the hysteresis has vanished. Salinity becomes nonzero when a critical point is reached, but the values change from zero continuously so the curve is characterized by a change in slope. Temperature shows a small change in slope at the same values of $\tilde{T}^*$. Density decreases monotonically with $\tilde{T}^*$.

The calculations were repeated for numerous other combinations of $\tilde{d}, \gamma$. The flow had multiple values in the range shown in Fig. 5. We see that in all cases $\gamma < 1$ for multiple states. This means that the resistance to flow of the top tube must be more than resistance of the bottom tubes. In addition, a broader range of tube resistance admits multiple equilibria as the upper layer is made progressively shallower ($\tilde{d} \to 0$). This means that a very shallow upper layer makes conditions more favorable for multiple equilibria.

5. Discussion

These are calculations of T–S multiple equilibrium in which the salinity field is simply quiescent stratified water. In contrast to the numerous studies that have been generated for oceanic climate models (reviewed by Marotzke, 1994, and Whitehead, 1995), or in thermosolutal systems (Turner, 1973; Tsitverblit, 1999), no salt-flux boundary condition is needed to accompany the heat flow boundary conditions. In addition, no complete reversal of the entire circulation cell characterizes the two opposing flow pattern. Although the flow in the middle tube changes sign, the flow is always from the top of the small basin to the bottom. In this sense, the two modes are less distinct from each other than the two modes in the earlier T–S multiple equilibrium models.

The implication for the ocean is that only the large layers of low-salinity water in polar oceans in conjunction with surface cooling are required to generate multi-equilibrium flows. No other boundary flux into the ocean such as atmospheric precipitation, wind mixing or river runoff is needed in addition to atmospheric cooling. The result is consistent with deep convection being

very dependent on the severity of wintertime cooling. During a mild winter only surface fresh water is cooled. In a severe winter the more saline deep water is cooled instead of relatively fresh surface water being more strongly cooled. A water mass of intermediate salinity is formed as a mixture of the saline water under the halocline and the fresher halocline water. This feature is also found in recent numerical models of thermohaline flows (Klinger and Marotzke, 1999). These results may therefore have some bearing on the formation of dense water as observed in the ocean (Gordon and Huber, 1990; Gordon et al., 1993; Lab Sea Group, 1998; MEDOC Group, 1969).

The effects depend on the three dimensionless parameters $\tilde{d}$, γ, and K. The fact that multiple equilibrium is found only for $\gamma < 1$ raises the question of whether this would also hold for more complex convection problems and whether the ocean would possess a value needed for multiple equilibria. Neither is answered by existing studies or data as far as we have determined. A more realistic model of deep ocean convection includes preconditioned currents that cause a doming of the deeper layers of cold salty water, baroclinic eddies that convey water in the deepened mixed layer away from the formation region, and an accurate equation of state for seawater, including pressure effects. Whether the surface halocline flows into the region of deep convection with more or less retardation than intermediate water is poorly understood at present to our knowledge. Possibly in the Arctic ocean, flow of fresh water under pack ice is retarded by the roughness, but in such regions, temperature is always close to the freezing point, and convection is dominated by salinity not temperature. Thus this model only highlights some possibilities that must be answered by further studies.

Acknowledgements

Support for this study was given by the Office of Naval Research under Grant N00014-99-1-0366. I thank G. Veronis for some suggestions. Contribution number 10342 of Woods Hole Oceanographic Institution.

References

Aagaard, K., Carmack, E.C., 1989. The role of sea ice and other fresh water in the Arctic Circulation. Journal of Geophysical Research 94, 14485–14498.

Gordon, A.L., Huber, B.A., 1990. Southern Ocean winter mixed layer. Journal of Geophysical Research 95, 11655–11672.

Gordon, A.L., Huber, B.A., Hellmer, H.H., Ffield, A., 1993. Deep and bottom water of the Weddell Sea's western rim. Science 262, 95–97.

Klinger, B., Marotzke, J., 1999. Behavior of double-hemisphere thermohaline flows in a single basin. Journal of Physical Oceanography 29, 382–399.

Lab Sea Group, 1998. The Labrador Sea Deep convection experiment. Bulletin of the American Meteorological Society 10, 2033–2058.

Legg, S., McWilliams, J.C., 2000. Temperature and salinity variability in heterogeneous oceanic convection. Journal of Physical Oceanography 30, 1188–1206.

Marotzke, J., 1994. Ocean models in climate problems. In: Malanotte-Rizzoli, P., Robinson, A.R. (Eds.), Ocean Processes in Climate Dynamics: Global and Mediterranean Example. Kluwer Academic Publishers, Dordrecht, pp. 79–109.

MEDOC Group, 1969. Observations of formation of deep water in the Mediterranean Sea. Nature 227, 1037–1040.
Stommel, H., 1962. On the smallness of sinking regions in the ocean. Proceedings of the National Academy of Sciences 48 (5), 766–772.
Sverdrup, H.U., Johnson, M.W., Fleming, R.H. (Ed.), 1942. The Ocean. Prentice-Hall, Englewood Cliffs, NJ, pp. 1087.
Tsitverblit, N., 1999. Multiplicity of equilibrium states in laterally heated thermosolutal systems with equal diffusivity coefficients. Physics of Fluids 11 (9), 2516–2538.
Turner, J.S. (Ed.), 1973. Buoyancy Effects in Fluids. Cambridge University Press, New York, pp. 367.
Whitehead, J.A., 1995. Thermohaline ocean processes and models. Annual Reviews of Fluid Mechanics 27, 89–113.